ISSN (Online) 2394-6849

International Journal of Engineering Research in Electronics and Communication Engineering (IJERECE)

Vol 11, Issue 8, August 2024

Electra MIMO Antenna Design for EV Wireless Communication

[1] Inderpreet Kaur, [2] Siddharth Bharti, [3] Vaibhav Singh, [4] Hari Kumar Singh

[1] [2] [3] [4] Department of Electronics and Communication Engineering, MJP Rohilkhand University Bareilly, India
Corresponding Author Email: [1] Inderpreet@mjpru.ac.in, [2] siddharth.btec45@mjpru.ac.in, [3] vaibhav.btec15@mjpru.ac.in, [4] hari.singh@mjpru.ac.in

Abstract*— The article presents the Electra MIMO antenna tailored for 5.7 GHz EV Wireless Communication. It showcases a slotted ring design with microstrip feeding, boasting a compact size of 25*25*1.6mm³ for a single element. The study delves into optimizing antenna performance by incorporating an extra circular ring with precise dimensions. This augmentation induces resonance via electrical lengthening, facilitated by an inductive effect. To tackle this, a ring-like structure is fashioned using a circular patch. This modification adeptly manages the antenna's single-band response and bandwidth by integrating corresponding slots into the modified circular patch.

Keywords*— MIMO Antenna, EV communication, Compact MIMO, MIMO Application.

I. INTRODUCTION

Patch antennas offer several benefits such as being lightweight, having a sleek profile, and being relatively simple to manufacture. They are particularly advantageous for automotive applications due to their built-in ground plane, which simplifies installation, especially on car roofs. For instance, in [1], a patch antenna housed within a shark-fin Radom is ideal for mounting on a car roof because of its compact size and performance capabilities. The patch antenna developed for automotive applications in [2] combines EV functionalities. It incorporates a main 4 circular ring patch and slot of square patch. Despite achieving some level of miniaturization by integrating modules, its 126 mm diameter presents difficulties in maintaining compactness. Integrating such antennas onto vehicles without compromising their appearance is a complex task. Designing antennas for vehicles involves considering various factors to ensure reliable and efficient communication systems while adhering to size constraints. Consequently, fitting multiple antennas into limited spaces presents a significant challenge [3].

Integrating MIMO Antenna (multiple input multiple output) into both 5G mobile networks and electronics vehicle applications is essential for fulfilling the demands of upcoming autonomous vehicle applications in the EV sector. MIMO Antenna, which utilize no of antennas at both ends of communication, offer enhancements in channel capacity, data rates, and overall system throughput without necessitating an expansion of frequency bands or an increase in transmit power. Nonetheless, crafting MIMO antennas for automotive usage encounters various hurdles, particularly concerning spatial constraints and interference among antennas housed within a single substrate. In MIMO Antenna challenges are the return loss, isolation and gain when placing the MIMO antennas, it is difficult to make an antenna system that fulfill criteria. Furthermore, the simultaneous integration of multiple applications like cellular 5G, GNSS, SDARS, and V2X communication systems within a unified package introduces additional complexities, including concerns regarding antenna size, interference, isolation, and operating bandwidth limitations. These factors are significantly influenced by the physical volume, complicating the design of efficient MIMO antenna systems. Determining the best positions for automotive antennas presents a challenge due to the intricate alterations in antenna behavior when mounted on vehicles. These changes encompass near-field phenomena of the radiation from the different obstacles, and some moving obstacles, all of which modify the intended current distributions. Despite these complexities, various studies have compared antenna positions on cars, with some identifying side mirrors, roof areas, and the front of the vehicle as promising locations based on performance assessments using ray tracing simulations.

II. ANTENNA DESIGNING

Figure 1 depicts the single antenna design of the single circular ring antenna. Situated at the top a thin FR4 (Substrate) with a permittivity of εr = 3.8 to 4.8 and a H(Thickness) = 1.6 mm of the radiating patch. The antenna's overall dimensions are 25x25x1.6. The coaxial probe delivers the radiating patch, which lies parallel to the y-axis, serving as the feed line in Design (1) of Fig 1. The outer shielding of the coaxial feed connects to both the upper circular radiating element and the lower rectangular ground plane of the antenna.

ISSN (Online) 2394-6849

International Journal of Engineering Research in Electronics and Communication Engineering (IJERECE)

Vol 11, Issue 8, August 2024

Table 1: Design Parameters of the Single Antenna

Parameters	Description	Dimensions (mm)
L	Length of Antenna	25mm
W	Width of Antenna	25mm
R1	Outer Radius of Patch	8mm
R2	Inner Radius of Patch	2mm
H	Height of Dielectric Substrate	1.6mm
L1	Gap between the circular patch	2mm

A. Evolution of single element of antenna

The initial design of the antenna begins with a circular patch, as depicted in Fig3. Design (2). In this Design, a 4-ring-shaped slot is connected to a feed line measuring 5x0.5 mm. This feed line is linked to a larger feed measuring 5.5x3.7 mm within the circular patch, aiming to achieve resonance at 5.7 GHz with relatively lower impedance matching compare. This resonance is facilitated by the inductive effect resulting from the electrical elongation induced by each circular ring. For counteract this inductive effect, a rectangular shape slot is subtracted from the circular ring. Additionally, another circular ring is introduced around the outer perimeter of the antenna, with an outer radius of 8 mm and the difference between two rings is the 0.5 mm, fully encompassing the four rings of the antenna, as depicted in Fig 1. Design (3). Incorporating this circular ring assists in controlling the single-band response and bandwidth of the antenna design. This is achieved by integrating specific slots into the modified circular patch, as outlined in the evolutionary process.

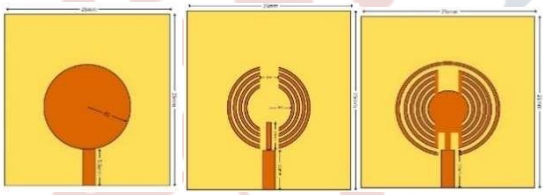

(a) (b) (c)

Fig1: Step wise antenna design (a) Design 1 (b) Design 2 (c) Design 3

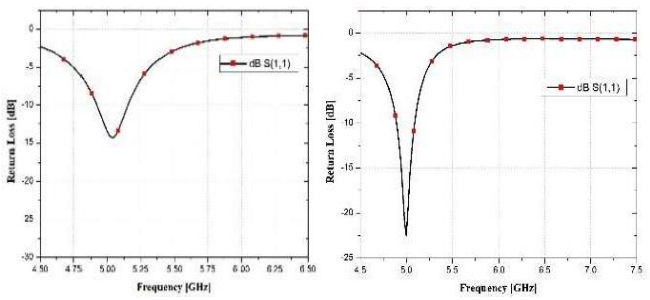

(a) (b)

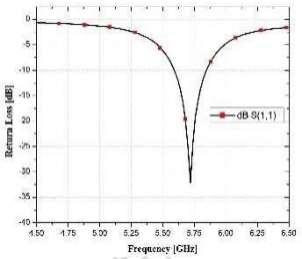

(c)

Fig1.1: Return Loss (a) Design 1 (b) Design 2 (c) Design3

III. PARAMETRIC ANALYSIS OF SINGLE ANTENNA

This section focuses on the design of a single antenna, conducting a detailed parametric analysis to explore key factors influencing its operation. Fig 5 displays how the radius (r) of the arc-shaped patch varies at different values. It's worth noting that optimal performance, indicated by the ||S11|| parameter, occurs when the radius is set at r1=8 mm.

The antenna design features a rectangular sub (25 × 25) positioned at the center of the arc-shaped patch, crucial for achieving a wide bandwidth within the desired frequency band. Fig 2 illustrates the variation of R1 at different values, showing that R1 = 2 mm yields the most favorable outcomes in terms of bandwidth. Notably, as R1 values increase, there's a noticeable downward shift in the S11 graph towards lower frequencies, with R2 = 8 mm demonstrating the best results in terms of Gain. Conversely, increasing R2 values lead to poor impedance matching, resulting in a shift towards higher magnitudes in the S11 graph. These findings offer valuable insights for optimizing antenna design to enhance performance.

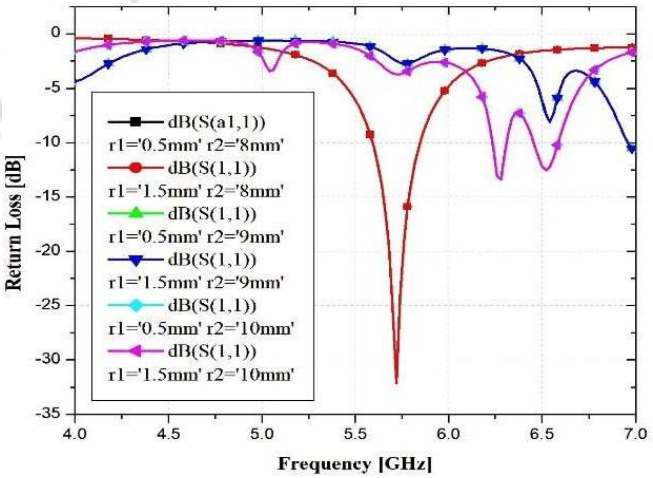

Fig 2. Return loss with variation of the radius.

ISSN (Online) 2394-6849

International Journal of Engineering Research in Electronics and Communication Engineering (IJERECE)

Vol 11, Issue 8, August 2024

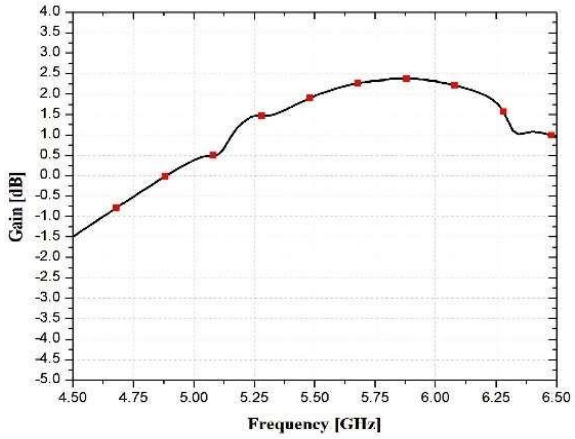

Fig 3. Gain of Single Antenna with the variation of the radius

A. Introducing MIMO Antenna Design

To make the performance of the single antenna design, a Multiple-Input Multiple-Output (MIMO) configuration is utilized. In Fig 4, Design (4) demonstrates the application of the parametric sweep technique to ascertain the optimal separation between antenna elements. Various spacing values are evaluated through simulations, and a separation distance (s) of 1.6 mm is the antenna's return loss and the isolation characteristics. The MIMO Antenna design and its isolation properties are illustrated accordingly. The isolation between antenna elements exceeds 40 dB, attributed to the presence of a planar ground structure [50, 50]. Additionally the MIMO antenna having the four antenna elements, with a gain of 1.7 dB and it is observed at the return loss at 5.7 GHz.

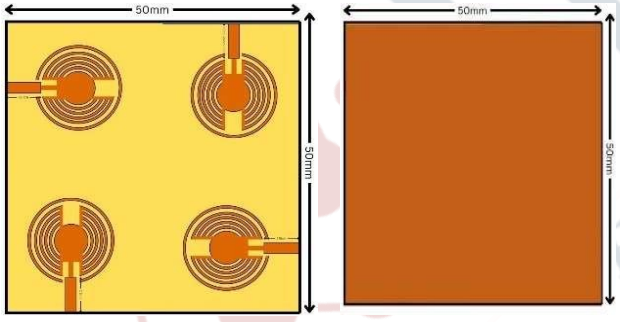

(a) (b)

Fig 4. MIMO Antenna, (a) Front view (b) Back view

IV. RESULTS

A four-ended MIMO Antenna incorporates a sequential feeding network achieved through suitable layout adjustments. This circularly polarized (CP) antenna's radiated section is constructed on a substrate of the H (Thickness) of 1.6 mm and a FR4 (relative permittivity) of 3.8 to 4.8, using sequential feeding. Front and back views of the antenna, which has a tin-coated dielectric substrate on five sides, are shown in Fig. 4 (Design 4).

A printed feeding network is positioned on one side, while a shared ground plane is situated on the other side. The antenna demonstrates an impedance bandwidth from 5.6 to 5.86 GHz, confirmed by ensuring S11 remains below −39 dB according to standard criteria Although achieving an impressive impedance bandwidth, evaluating diversity gain is essential to assess the performance of the MIMO antenna. By comparing the signal received by the desired antenna element with the signal received by a combination of other elements, diversity gain quantifies the strength of the signal of the MIMO antenna. After analysis, it is shown that the suggested MIMO antenna has a simulated diversity gain of about 1.6 dB.

A. Scattering Performance

Figures 5a and 5b displays the resulting four-port array. Corresponding reflection and isolation parameters are depicted in Figures 5a and 5b. Figure 5a illustrates that adding two more elements renders the circuit inductive and shifts the resonance towards the right side. Finally, two additional pairs are symmetrically incorporated, forming an eight-port MIMO array as depicted in Figure 5c. In this configuration, the orthogonal elements demonstrate good isolation of over 20 dB without the need for any decoupling structure.

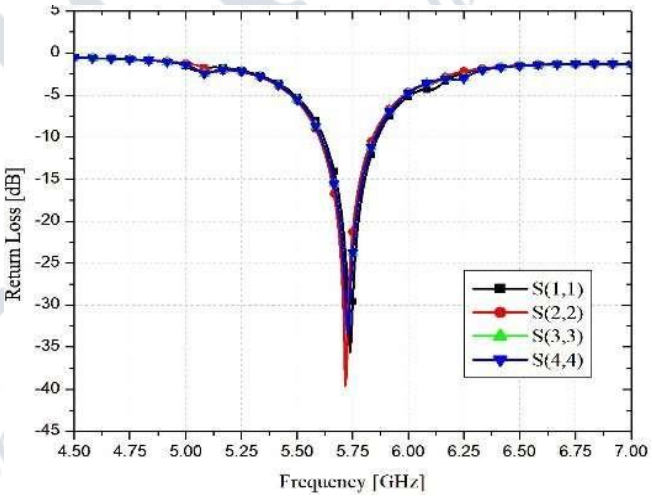

(a)

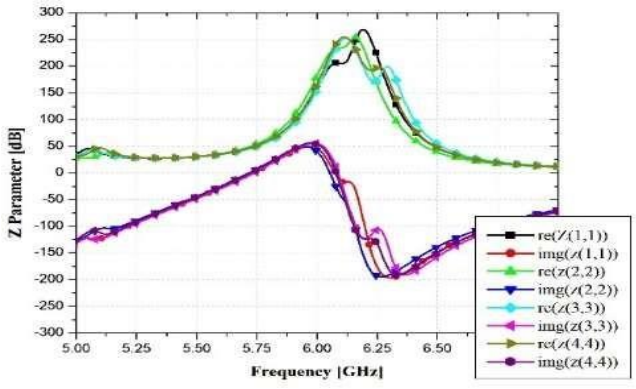

(a)

ISSN (Online) 2394-6849

International Journal of Engineering Research in Electronics and Communication Engineering (IJERECE)

Vol 11, Issue 8, August 2024

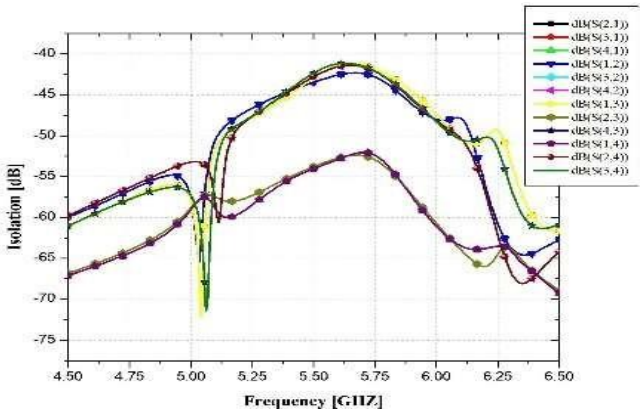

(b)

Fig.5. (a) Reflection Coefficient (b) Z Parameter

B. Radiation performance

The antenna exhibits a broadside radiation pattern directed towards the +z direction. Figure 6. displays simulated radiation patterns in the xz-plane and yz-plane for excitation at all ports.

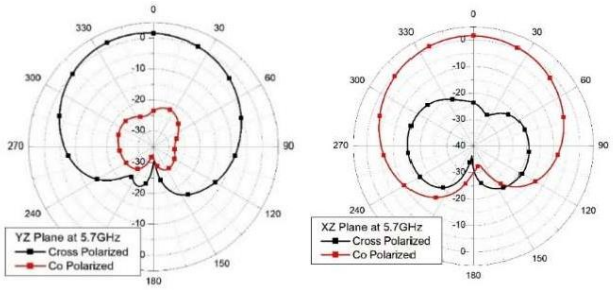

(a) (b)

Fig.6. Radiation Pattern (a) YZ Plane (b) XZ Plane

C. Diversity Performance

The Equivalent Coupling Coefficient (ECC) quantifies how closely the radiation pattern of one antenna aligns with that of another when they are employed nearby. A high ECC value detrimentally affects the MIMO performance of the antenna. Typically, for optimal MIMO operation, it is recommended to maintain an ECC value below 0.5.. ECC is calculated using the S parameter as

$$ECC = \rho(i,j,N) = \frac{\left|\left(\sum_{n=1}^{N}\{S_{in}^{*}S_{nj}\}\right)\right|^{2}}{\prod_{k=i,j}\left(1-\sum_{n=1}^{N}\{S_{kn}^{*}S_{nk}\}\right)} \quad (1)$$

Where i, j are any two ports and N=8(1) The MIMO antenna's diversity performance is demonstrated by DG, which may be assessed using ECC.

$$DG = 10\sqrt{(1-|ECC|^{2})} \quad (2)$$

Figs. 7. a and b depict simulated ECC and DG charts. It can be seen that for 5.9GHz, the DG is greater than 9.8 dB and the ECC results are significantly below 0.18.

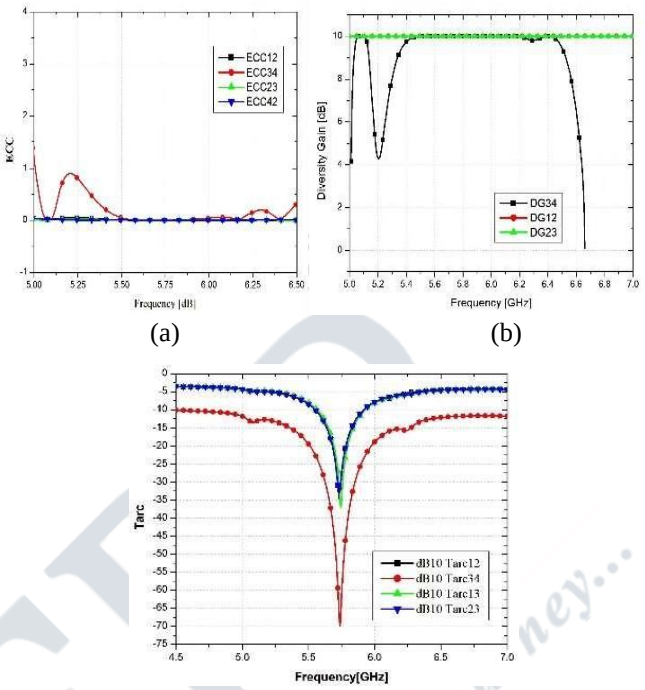

(a) (b)

(c)

Fig.7. (a) ECC, (b) DG (c) TARC

D. Surface Current Distribution

In Fig 8 displays the electric field patterns. It is evident that when all ports are activated, the isolation between the antennas is notably deficient, as depicted in Figure 8a. The surface current distribution illustrates this inadequacy confirms this lack of isolation.

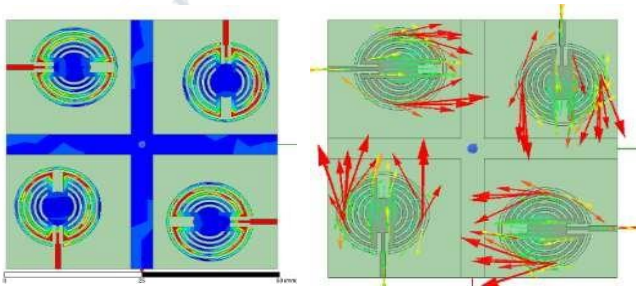

(a) (b)

Fig.8. Surface Current Distribution at 5.7 GHz (a) and (b)

E. Group Delay

Here, Fig 9 depicts the group delay of the proposed structure, which represents the duration for a signal input at the antenna feed location to traverse through the matching network, radiating element, and device packaging before being emitted into free space. In MIMO antennas, group delay can indicate errors caused by multiple reflections due to the proximity of elements. By exciting two identical antennas facing each other in the far field, it is noted that the measured group delay stays consistent across the current band. Notable peaks are observed in the group delay at the notch bands.

ISSN (Online) 2394-6849

International Journal of Engineering Research in Electronics and Communication Engineering (IJERECE)

Vol 11, Issue 8, August 2024

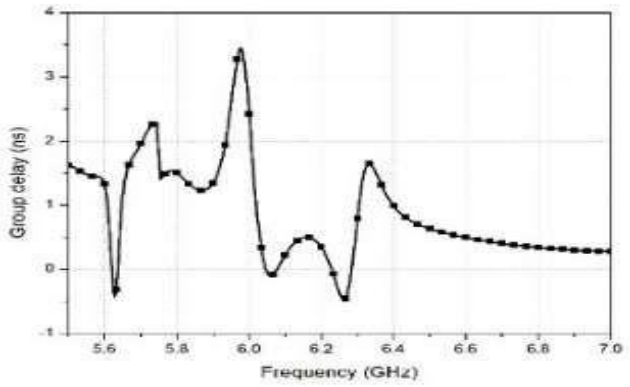

Fig.9. Group Delay

REFERENCES

[1] M. O. Khalifa, A. M. Yacoub and D. N. Aloi, "A Multiwideband Compact Antenna Design for Vehicular Sub-6 GHz 5G Wireless Systems," in IEEE Transactions on Antennas and Propagation, vol. 69, no. 12, pp. 8136-8142, Dec. 2021, doi: 10.1109/TAP.2021.3083770.

[2] M. M. Bilgic and K. Yegin, ‘‘Modified annular ring antenna for GPS and SDARS automotive applications,’’ IEEE Antennas Wireless Propag. Lett., vol. 15, pp. 1442–1445, 2016.

[3] G. Artner, W. Kotterman, G. Del Galdo and M. A. Hein, "Automotive Antenna Roof for Cooperative Connected Driving," in IEEE Access, vol. 7, pp. 20083-20090, 2019, doi: 10.1109/ACCESS.2019.2897219.

[4] S. Kumar, A. S. Dixit, R. R. Malekar, H. D. Raut, and L. K. Shevada, “Fifth generation antennas: a comprehensive review of design and performance enhancement techniques,” IEEE Access, vol. 8, pp. 163568–163593, 2020.

[5] M. Alibakhshikenari, B. S. Virdee, C. H. See et al., “Dualpolarized highly folded bowtie antenna with slotted selfgrounded structure for sub-6 GHz 5G applications,” IEEE Transactions on Antennas and Propagation, vol. 70, no. 4, pp. 3028–3033, 2022

[6] M. Alibakhshikenari, B. S. Virdee, A. A. Althuwayb et al., “Study on on-chip antenna design based on metamaterialinspired and substrate- integrated waveguide properties for millimetre-wave and THz integrated-circuit applications,” Journal of Infrared, Millimeter and Terahertz Waves, vol. 42, no. 1, pp. 17–28, 2021.

[7] J. d. D. Ntawangaheza, L. Sun, Z. Xie, Y. Pang, Z. Zheng, and G. Rushingabigwi, “A single-layer low-profle broadband metasurface antenna array for sub-6 GHz 5G communication systems,” IEEE Transactions on Antennas and Propagation, vol. 69, no. 4, pp. 2061– 2071, 2021.

[8] Z. Shao and Y. Zhang, “A single-layer miniaturized patch antenna based on coupled microstrips,” IEEE Antennas and Wireless Propagation Letters, vol. 20, no. 5, pp. 823–827, 2021.

[9] P. Sambandam, M. Kanagasabai, R. Natarajan, M. G. N. Alsath, and S. Palaniswamy, “Miniaturized buttonlike WBAN antenna for of-body communication,” IEEE Transactions on Antennas and Propagation, vol. 68, no. 7, pp. 5228–5235, July 2020.

[10] J. d. D. Ntawangaheza, L. Sun, Y. Li, D. Biao, Z. Xie, and G. Rushingabigwi, “A single-layer planar low-profle wideband microstrip line-fed metasurface antenna,” IEEE Antennas and Wireless Propagation Letters, vol. 20, no. 9, pp. 1641–1645, Sept. 2021.

[11] M. O. Khalifa, A. M. Yacoub, and D. N. Aloi, “A multiwideband compact antenna design for vehicular sub-6GHz 5G wireless systems,” IEEE Transactions on Antennas and Propagation, vol. 69, no. 12, pp. 8136–8142, 2021.

[12] N. Hussain and N. Kim, “Integrated microwave and mm-wave MIMO antenna module with 360 pattern diversity for 5G internet-of-things,” IEEE Internet of Tings Journal, p. 1, 2022.